Optimal Allocation Strategy for Electric EPSVs and Hydrogen Fuel Cell EPSVs Balancing Resilience and Economics

Wei Tang, *Member*, *IEEE*, *CSEE*, Zhaoqi Wang, *Member*, *IEEE*, Lu Zhang, *Member*, *IEEE*, *CSEE*, Bo Zhang, *Member*, *IEEE*, Jun Liang, *Fellow*, *IEEE*, Keyan Liu, *Member*, *IEEE*, and Wanxing Sheng, *Senior Member*, *IEEE*

***Abstract*—Distribution networks (DNs) face challenges in maintaining continuous power supply for critical loads under disasters. However, from a resilience perspective, the forecast accuracy of line/component failure rates under hurricanes still needs to be improved in order to gain an optimal allocation strategy for multiple emergency power supply vehicles (EPSVs), and the economics under normal state is supposed to be considered in the optimization pre-hurricane EPSV allocation. Due to the rapid development of environmentally friendly EPSVs, electric EPSVs and hydrogen fuel cell EPSVs are considered to be allocated jointly for their different advantages in enhancing DNs' resilience. Hence, to balance the resilience and economics of DNs against hurricanes, an equilibrium allocation strategy for electric EPSVs and hydrogen fuel cell EPSVs is proposed in this paper based on the Nash equilibrium. First, a statistical model for meteorological data about hurricanes is established via the conditional value at risk (CVaR) considering strong wind and the consequent rainfall. Failure rate models of DN lines/components are built on account of the damage mechanism of hurricanes. Then the emergency power supply capability of electric EPSVs and hydrogen fuel cell EPSVs are calculated considering the limited power energy stored in electric EPSVs and abundant hydrogen in a hydrogen fueling station. In addition, an equilibrium allocation strategy for sizing and locating multiple EPSVs is proposed, in which the Nash equilibrium method is utilized. Finally, simulation tests verify the superiority of the proposed failure rate models and equilibrium allocation strategy in balancing the resilience of DNs under hurricanes and the economics of DNs under normal states.**

***Index Terms*—Distribution network, economics, electric emergency power supply vehicle, hydrogen fuel cell emergency power supply vehicle, Nash equilibrium, resilience.**

I. Introduction

EXTREME natural disasters, such as hurricanes, usually cause severe damage to distribution networks (DNs), and then huge structural damage and long-term large-scale power outages appear as a result of high wind speed and strong rainfall intensity [1], [2]. To improve resilience indicating the ability of DNs to prevent high-impact low-probability (HILP) events and quick restoration of power supply, an accurate prediction of DN failure rates and optimal allocation of emergency power supply sources are considered major roles in pre-hurricane DN planning.

Emergency power supply vehicles (EPSVs) [3] have been allocated as effective measures to guarantee continuous power supply under disasters, especially electric EPSVs, but overinvestment may occur if excessive EPSVs are allocated for low-probability events. On the other hand, insufficient EPSVs will delay DN restoration under disasters, which may cause huge economic losses especially for critical loads. Moreover, hydrogen fuel cell EPSVs have been developing vigorously for the booming growth of hydrogen fueling stations to provide abundant hydrogen locally after disasters [4], and are utilized to maintain continuous power supply under hurricane Shanzhu in Zhejiang Province of China. Therefore, it is of great significance to allocate electric EPSVs and hydrogen fuel cell EPSVs, jointly, before disasters considering the complementarity between the above two types of EPSVs, so outage power loss can be reduced, and overinvestment can be avoided. However, there are two critical challenges in sizing and locating EPSVs to minimize outage power losses with the lowest investment. One is the accurate evaluation of the failure rates of DNs, the other is the equilibrium between resilience and economics of DNs considering different characteristics in power supply of multiple EPSVs.

In order to allocate emergency power supply sources properly for maintaining continuous power supply for critical loads, the accuracy of failure rate evaluation in DNs is considered a critical basis. Historical data were utilized in [5] to establish meteorological models under floods and earthquakes. However, due to the low probability of extreme natural disasters, the accuracy of the disaster model based on a small amount of historical data can hardly meet the requirements. To improve prediction accuracy, a Monte Carlo method was used to expand the sample size and hence a probability model was established

Manuscript received July 26, 2021; revised September 23, 2021; accepted October 12, 2021. Date of online publication August 18, 2022; date of current version September 14, 2022. This work was supported by Funds for International Cooperation and Exchange of the National Natural Science Foundation of China (Grant No. 52061635104).

W. Tang, L. Zhang (corresponding author, email: zhanglul@cau.edu.cn; ORCID: https://orcid.org/0000-0001-5696-2418) and B. Zhang are with the College of Information and Electrical Engineering, China Agricultural University, Beijing 100083, China.

Z. Q. Wang is with State Grid Energy Research Institute Co. Ltd, Beijing 102209, China.

J. Liang is with the School of Engineering, Cardiff University, Cardiff CF24 3AA, U.K.

K. Y. Liu and W. X. Sheng are with China Electric Power Research Institute, Beijing 100192, China.

DOI: 10.17775/CSEEJPES.2021.05430

[6]. Afterwards, the conditional value at risk (CVaR) was further proposed to describe the conditional mean of the probability distribution functions (PDFs) of meteorological models with a confidence interval of 95% in [7], which makes the disaster models more conservative and reliable. Furthermore, the application of CVaR can overcome insufficiency of the value at risk (VaR) for tail estimation based on additivity, positive homogeneity, monotonicity and transfer invariance. However, the above statistical models can only depict the intensity of disasters at a specific moment, lacking the capability of reflecting time variations of disasters. Therefore, a time-variable model was proposed in [8] to characterize the intensity of disasters at any moment of dynamic disaster duration. However, the existing statistical models of hurricanes [9] only describe the instantaneous wind speed without considering rainfall and hurricane durations. This may affect accuracy of line/component failure rate models of DNs, thereafter, the rationality of multiple EPSV allocation results will be weakened.

Existing research usually concentrated on proposing an optimized allocation strategy of emergency power supply sources of DNs [10]–[12]. Different types of emergency power supply sources were also allocated to enhance the resilience of DNs, such as distributed generators (DGs) and EPSVs. For example, the mixed integer programming method, piecewise linearization method and robust optimization method were implemented to obtain the allocation results of DGs in [13], [14]. However, DGs are usually located at fixed locations, indicating the power supplies provide little maneuverability or mobility under disasters. Moreover, the output power of DGs is greatly affected by meteorological factors, hence it is difficult to ensure a continuous power supply for critical loads under extreme natural disasters. To overcome the above shortcomings of DGs which resulted in quite complex optimization problems, a bi-level mixed integer programming model and a quadratic curve optimization model were established in [15]. In the novel AC/DC hybrid DNs [16], taking EPSVs as emergency power supply sources is another solution without increasing the complexity of optimization models. Mobile emergency generators and devices were considered as useful measures to enhance resilience under ice storms and other natural disasters, and the routing of emergency vehicles were further discussed in [17], [18]. However, existing research mainly dealt with dispatching strategies during restoration periods with little consideration of the sizing and locating of EPSVs [19], [20]. In addition, existing pre-hurricane DN planning strategies only enhanced the resilience of DNs while hardly considering the economic aspects [21]. For example, reference [22] evaluated the resilience of DNs based on an optimization allocation method during the period of prevention, survival and restoration without calculating the economics. As extreme natural disasters are low-probability events, overinvestment will be caused if a large amount of emergency power supply sources are allocated.

To mitigate the above shortcomings, time-variable probability models of wind speed and rainfall caused by hurricanes are proposed in Section III during the whole hurricane duration. On this basis, failure rates of DNs under hurricanes can be evaluated accurately combined with damage mechanisms of DN components. Then allocating electric EPSVs and hydrogen fuel cell EPSVs jointly, where their different capabilities in maintaining continuous power supply of critical loads are considered Section IV. The capabilities of electric EPSVs are determined by maximum output power and capacities, but hydrogen fuel cell EPSVs are only correlated with maximum output power because hydrogen can be replenished in a hydrogen fueling station during the restoration period. In Section V, a multi-objective optimization allocation strategy portrays inconsistent variation trends between resilience and economics through the lens of DNs. By defining the resilience and economics of DNs as two players utilizing the Nash equilibrium method, an equilibrium model is obtained to transform the above multi-objective optimization to a single-objective one. Note that the Nash equilibrium method has been widely used for solving power restoration problems considering various conflicting objectives and constraints [23]–[25]. Then, a Pareto-based non-dominated sorting genetic algorithm II (NSGA-II) is applied for solving the proposed multi-objective optimization model, and then the equilibrium point of Pareto frontier is obtained by the above Nash equilibrium method and genetic algorithm (GA). Section VI presents case studies on an IEEE 33-node DN in hurricane-prone areas to verify the proposed failure rate models under hurricanes and the equilibrium strategy of resilience and economics. Finally, conclusions are summarized in Section VII.

II. Problem Description and Framework

To ensure continuous power supply for critical loads under hurricanes, it is of great significance to propose an optimal allocation strategy of multiple EPSVs. However, failure rates of DNs under hurricanes caused by wind speed and rainfall intensity jointly, are hard to describe by traditional probability models. During the whole planning period considering hurricanes, dynamic dispatching of EPSVs due to their different power supply capabilities and mobility also need to be considered to ensure continuous power supply of prioritized critical loads.

There is still another key point lying in the allocation strategy of EPSVs considering hurricanes owing to their low probability characteristics, where the equilibrium between resilience under hurricanes and economics under normal states is necessary to be further stated. However, it is difficult to fully utilize the emergency power supply capabilities of electric EPSVs and hydrogen fuel cell EPSVs during the restoration period after hurricanes. It is also hard to transform a multi-objective optimization model into a single-objective one by the existing entropy weight method as outage losses and economic benefits are two goals with inconsistent variation trends. Therefore, it is significant to evaluate temporal output powers and capacities of multiple EPSVs and portray the bargaining process towards resilience and economics via the game theory, such as the Nash equilibrium method, because the game theory can reflect the diversity of dimensions, magnitudes and probabilities between players.

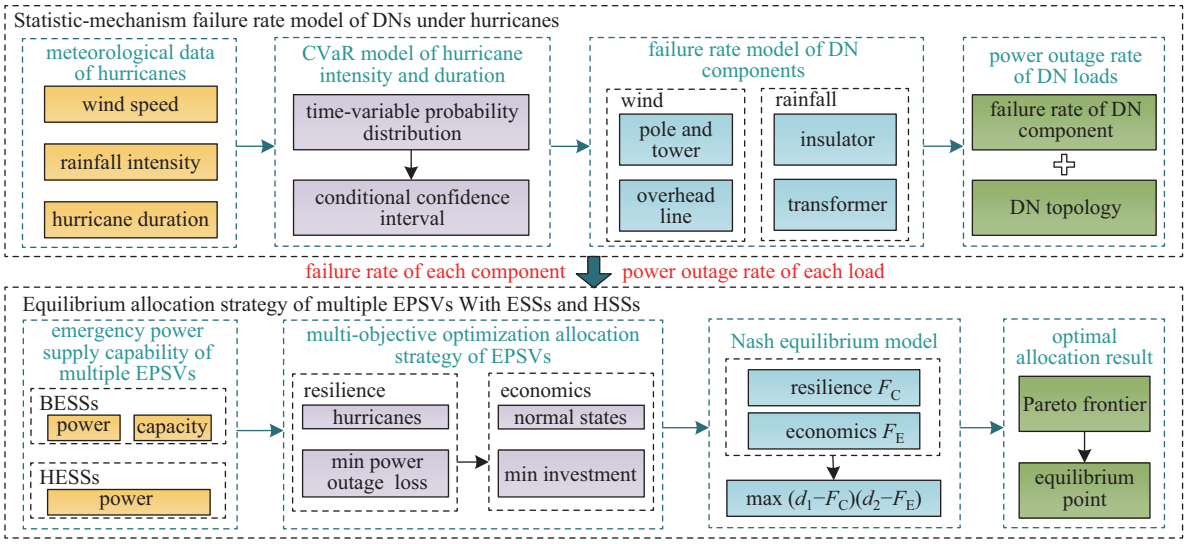

Fig. 1. Framework of the proposed equilibrium allocation strategy of multiple EPSVs considering hurricanes.

As shown in Fig. 1, dealing with the above critical points, through the lens of the resilience under hurricanes and economics under normal states, an optimal pre-hurricane.1allocation method of multiple EPSVs is proposed based on the Nash equilibrium method. The framework of the proposed allocation strategy is as follows:

a) Statistic-mechanism failure rate model of DNs under hurricanes. The intensity and duration of hurricanes are modeled in Section III CVaR based on additivity, positive homogeneity, monotonicity and transfer invariance, where probability distributions of wind speed, rainfall intensity and hurricane duration are obtained by PDFs considering the uncertainty of hurricanes. Line/component failure rates in DNs are further modeled by analyzing the effects of wind speed, rainfall intensity and hurricane duration on DN components, which mainly contain broken lines, collapsed poles/towers, insulators and transformers; on this basis, failure rate models are established. Assuming that various failures of DN components are independent, power outage rates of loads in DNs are gained considering DN topologies.

b) Optimization allocation strategy of electric EPSVs and hydrogen fuel cell EPSVs via Nash equilibrium. In Section IV, emergency power supply capabilities of electric EPSVs and hydrogen fuel cell EPSVs are evaluated. A multi-objective optimization model is established considering resilience under hurricanes and economics under normal states in Section V. Note that resilience is represented by the outage cost under hurricanes, and economics is correlated with investment cost, maintenance cost and reliability improvement by EPSVs. Then, to seek for the optimal sizing and locating solution of EPSVs balancing the above two objectives, the Nash equilibrium method is adopted to transform the multi-objective optimization to a single-objective one, for its superiority in dealing with multiple inconsistent objectives based on linear transformation invariance principle, so an optimal pre-hurricane allocation strategy of multiple EPSVs can be obtained.

III. Statistic-Mechanism Failure Rate Model of DNs Under Hurricanes

The line/component failure rates of DNs will increase significantly under strong wind and rainfall, which mainly is caused by the following two aspects: one is it will lead to collapsed poles/towers and broken lines once the wind load exceeds the load capacities of poles, towers and overhead lines; the other is a decrease of resistance on the surface of insulators and transformers caused by strong rainfall will lead to insulators flashing and insulation failures of transformers. Failure rate models of lines and components in DNs, such as poles, towers, overhead lines, insulators and transformers, are established in this section considering strong hurricanes and consequent rainfall.

A. CVaR Models of Meteorological Factors Under Hurricanes

To precisely model meteorological factors of hurricane intensity and duration, PDFs characterizing wind speed and rainfall intensity are obtained based on the fitted curves of historical meteorological factors, and then confidence intervals are obtained by establishing CVaR models. The end of a hurricane is determined by the moment when the wind speed decreases to 12 on the Beaufort Scale [26].

Time-variable probability vectors of wind speed and rainfall intensity can be expressed as:

$$V(t) = \begin{bmatrix} V_{\text{wind}}(t) & V_{\text{rain}}(t) \end{bmatrix} \tag{1}$$

where $V_{\text{wind}}(t)$ is the probability vector of wind speed at moment t, and $V_{\text{rain}}(t)$ is the probability vector of rainfall intensity at moment t.

The PDF of $V(t)$ is defined as $\rho(V(t))$, which can be obtained by fitting historical data of wind speed and rainfall intensity [7]. The conditional confidence interval $[R^{\text{low}}_{\text{CVaR}}, R^{\text{up}}_{\text{CVaR}}]$ is obtained with a confidence coefficient β. The CVaRs are

$$R^{\text{up}}_{\text{CVaR}} = \frac{1}{1-\beta} \int_{V(t) \geq R^{\text{up}}_{\text{VaR}}(t)} V(t)\rho(V(t))\mathrm{d}(V(t))$$

$$R_{\mathrm{CVaR}}^{\mathrm{low}}=\frac{1}{1-\beta}\int_{V(t)\le R_{\mathrm{VaR}}^{\mathrm{low}}(t)}V(t)\rho(V(t))\mathrm{d}(V(t)) \quad (2)$$

where $R_{\mathrm{VaR}}^{\mathrm{up}}$ and $R_{\mathrm{VaR}}^{\mathrm{low}}$ are the critical values of the conditional confidence interval, which can be defined as:

$$\begin{cases} R_{\mathrm{VaR}}^{\mathrm{up}}=\min\left\{\alpha\in R:\phi^{\mathrm{up}}\ge\beta;\right. \\ \qquad\left.\phi^{\mathrm{up}}(\alpha)=\displaystyle\int_{V(t)\le\alpha}\rho(V(t))\mathrm{d}(V(t))\right\} \\ R_{\mathrm{VaR}}^{\mathrm{low}}=\min\left\{\alpha\in R:\phi^{\mathrm{low}}\ge\beta;\right. \\ \qquad\left.\phi^{\mathrm{low}}(\alpha)=\displaystyle\int_{V(t)\ge\alpha}\rho(V(t))\mathrm{d}(V(t))\right\} \end{cases} \quad (3)$$

where ϕ^{up} and ϕ^{low} are the probabilities that $V(t)$ is outside the threshold α at moment t.

The hurricane duration T can be expressed as:

$$T=t_{\mathrm{end}}-t_{\mathrm{begin}}\in[t_{\mathrm{end}}^{\mathrm{low}}-t_{\mathrm{begin}},t_{\mathrm{end}}^{\mathrm{up}}-t_{\mathrm{begin}}] \quad (4)$$

where t_{begin} is the initial time of hurricanes and t_{end} is the terminal time of hurricanes. The boundaries of the confidence interval $t_{\mathrm{end}}^{\mathrm{up}}$ and $t_{\mathrm{end}}^{\mathrm{low}}$ can be obtained by (5).

$$\begin{cases} t_{\mathrm{end}}^{\mathrm{up}}=\min\{t;V_{\mathrm{wind}}^{\mathrm{up}}(t)\le V_{w\min}\&\&V_{\mathrm{rain}}^{\mathrm{up}}(t)\le V_{r\min}\} \\ t_{\mathrm{end}}^{\mathrm{low}}=\min\{t;V_{\mathrm{wind}}^{\mathrm{low}}(t)\le V_{w\min}\&\&V_{\mathrm{rain}}^{\mathrm{low}}(t)\le V_{r\min}\} \end{cases} \quad (5)$$

where $V_{\mathrm{wind}}^{\mathrm{up}}$ and $V_{\mathrm{rain}}^{\mathrm{up}}$ are the upper boundaries of the confidence intervals of wind speed and rainfall intensity; $V_{\mathrm{wind}}^{\mathrm{low}}$ and $V_{\mathrm{rain}}^{\mathrm{low}}$ are the lower boundaries of the confidence intervals of wind speed and rainfall intensity; $V_{w\min}$ is the minimum value of wind speed; $V_{r\min}$ is the minimum value of rainfall intensity.

t_{total} is defined to show the outage time of loads under hurricanes, which can be expressed by the confidence interval of hurricane duration.

$$t_{\mathrm{total}}=\frac{(t_{\mathrm{end}}^{\mathrm{low}}-t_{\mathrm{begin}})+(t_{\mathrm{end}}^{\mathrm{up}}-t_{\mathrm{begin}})}{2} \quad (6)$$

B. Failure Rates of DN Components Under Wind Loads

The direct impact of hurricanes on DNs is characterized as effects on poles and towers. By calculating the wind load on poles, towers and overhead lines under hurricanes, failure rate models correlated with wind speed are developed [27].

1) Wind Load Effects for Poles, Towers and Overhead Lines

At moment t during hurricanes, the wind speed at point P can be expressed as:

$$V_P(t)=\begin{cases} V_{\mathrm{wind}}(t) & L_P\in[0,R_{\mathrm{eye}}] \\ \dfrac{V_{\mathrm{wind}}(t)R_{\mathrm{eye}}}{L_P} & L_P\in[R_{\mathrm{eye}},\infty] \end{cases} \quad (7)$$

where $V_{\mathrm{wind}}(t)$ is the wind speed of hurricanes at moment t; R_{eye} is the radius of the hurricane; and L_P is the distance between the hurricane center and point P.

Wind load at point P can be expressed as the sum of the wind loads on lines, poles/towers and insulators at moment t, i.e., $w_{\mathrm{x}}(t)$, $w_{\mathrm{s}}(t)$ and $w_{\mathrm{z}}(t)$, respectively.

$$\begin{aligned} w_{\mathrm{x}}(t)&=\alpha\mu_{\mathrm{z}}\mu_{\mathrm{SC}}dl_{\mathrm{H}}\sin^2\varphi\frac{V_P(t)^2}{1600} \\ w_{\mathrm{s}}(t)&=\beta\mu_{\mathrm{z}}\mu_{\mathrm{S}}A\frac{V_P(t)^2}{1600} \\ w_{\mathrm{z}}(t)&=n_1n_2\mu_{\mathrm{z}}A_{\mathrm{P}}\frac{V_P(t)^2}{1600} \end{aligned} \quad (8)$$

where α is the uneven coefficient of wind pressure on overhead lines; μ_{z} is the coefficient of wind pressure depending on height; μ_{SC} is the shape coefficient of overhead lines; d is the outer diameter of overhead lines; l_{H} is the horizontal span; φ is the angle between the wind and overhead lines; β is the vibration coefficient of the wind; μ_{S} is the shape coefficient of wind loads; A is the windward projected area of poles and towers; n_1 is the number of insulator strings on a single-phase line; n_2 is the number of insulators on each insulator string; and A_{P} is the windward area of each insulator.

The cross-bending of poles and towers at moment t is:

$$\begin{aligned} &M_{\mathrm{X}}(t)=(w_{\mathrm{xz}}(t)h_1+w_{\mathrm{sv}}(t)h_1\overline{h})\cdot(1+m_{\mathrm{x}}) \\ &\text{with}\begin{cases} w_{\mathrm{xz}}(t)=w_{\mathrm{x}}(t)+w_{\mathrm{z}}(t) \\ w_{\mathrm{sv}}(t)=\beta\mu_{\mathrm{z}}\mu_{\mathrm{s}}F\dfrac{V_P(t)^2}{1600} \\ \overline{h}=\dfrac{h_1}{3}\cdot\dfrac{2D_0+D_{\mathrm{x}}}{D}_0+D_{\mathrm{x}} \end{cases} \end{aligned} \quad (9)$$

where $w_{\mathrm{xz}}(t)$ is the sum of wind loads on lines and insulators; $w_{\mathrm{sv}}(t)$ is the sum of wind loads on poles and insulators; h_1 is the distance from a certain cross to the top of poles; $\overline{h}$ is the distance from a certain cross to the wind pressure point; m_{x} is the additional bending moment coefficient caused by the disturbance; F is the windward projected area of poles and towers; D_0 is the tip diameter of poles and towers; and D_{x} is the cross diameter of poles and towers.

2) Failure Rate Models of Poles and Towers

During hurricanes, once cross-bending exceeds the cross-bending strength of poles and towers, poles/towers will collapse. To describe the failure rate of poles and towers, a state function of poles and towers is proposed, see (9).

$$Z=R-S \quad (10)$$

where R is the bending strength of poles and towers as shown in (11), which follows the Gaussian; and S is the inner stress of poles and towers caused by wind loads, which is related to the speed and direction of the wind.

$$\begin{aligned} &f_{\mathrm{r}}(R)=\frac{1}{\sqrt{2\pi}\delta_{\mathrm{P}}}\mathrm{e}^{-\frac{1}{2}(\frac{R-\mu_{\mathrm{P}}}{\delta}{}_{\mathrm{P}})^2} \\ &\text{with}\begin{cases} \mu_{\mathrm{P}}=\beta M_{\mathrm{u}} \\ \delta_{\mathrm{P}}=\upsilon M_{\mathrm{u}} \end{cases} \end{aligned} \quad (11)$$

where μ_{P} is the mean value of the bending strength of poles and towers; δ_{P} is the standard deviation of the bending strength of poles and towers; β and υ are constants which can be measured by operating experience or destructive tests; and M_{u} is the capacity of bearing wind loads of poles and towers.

Thus, the stable operation probability for poles and towers is:

$$P(t)=P\{(R-S)>0\}=\int_0^{\infty}f_{\mathrm{r}}(R)\mathrm{d}R \quad (12)$$

The failure rate of poles and towers can be described as:

$$P_{\mathrm{r}}(t)=1-P(t)=\int_0^S \frac{1}{\sqrt{2\pi}\delta_{\mathrm{p}}}\mathrm{e}^{-\frac{1}{2}(\frac{R-\mu_{\mathrm{p}}}{\delta_{\mathrm{p}}})^2}\mathrm{d}R \tag{13}$$

3) Failure Rate Models of Overhead Lines

Overhead lines will break once bending exceeds the cross-bending strength, which is similar with failure rate models. To describe the failure rate of overhead lines, the self-weight L_{G} and maximum stress L_{Desm} of overhead lines can be calculated as:

$$\begin{cases} L_{\mathrm{G}}=L_{\mathrm{v}}G_0 g \\ L_{\mathrm{Desm}}=\dfrac{0.6T_{\mathrm{m}}}{K} \end{cases} \tag{14}$$

where L_{v} is the vertical span between overhead lines; G_0 is the mass of overhead lines per meter; T_{m} is the breaking force determined by the type of overhead lines; and K is the safety factor.

The state function of overhead lines can also be obtained as given in (10), in which S can be expressed as:

$$S=L_{\mathrm{G}}+L_{\mathrm{Desm}} \tag{15}$$

Therefore, the failure rate of overhead lines is:

$$P_{\mathrm{l}}(\mathrm{t})=\int_0^S \frac{1}{\sqrt{2\pi}\delta_{\mathrm{p}}}e^{-\frac{1}{2}(\frac{R-\mu_{\mathrm{p}}}{\delta_{\mathrm{p}}})^2}\mathrm{d}R \tag{16}$$

where R is the tensile strength of overhead lines; μ_{P} is the average of R; and δ_{P} is the standard deviation of R.

C. Failure Rates of DN Components Under Rainfall Loads

The indirect impact of hurricanes on DNs is characterized as effects on insulators and transformers caused by heavy rainfall. To describe these effects, failure rate models of insulators and transformers related to rainfall intensity and duration are developed [28].

1) Failure Rate Models of Insulators

Once insulators are submerged in water, a short circuit will occur leading to a power outage in DNs. Under heavy rainfall, insulator flashover is one of the main causes of outages.

Critical rainfall intensity of insulators can be expressed as [29]:

$$A_{\varsigma}=\left\{\frac{\ln[U_{\varsigma}/a(P/P_0)-b]}{cP}\right\}^{-\frac{1}{0.055}}-0.02 \tag{17}$$

where U_{ς} is the critical flashover voltage of insulators; P is the ambient atmospheric pressure; P_0 is the standard atmospheric pressure; and a, b and c are constant coefficients with the values of 2.021, 2.981 and 0.0003.

The flashover probability of each insulator is:

$$P_{\mathrm{i}}(t)=1-\int_0^{A_{\varsigma}} F(V_{\mathrm{rain}}(t))\mathrm{d}V_{\mathrm{rain}}(t) \tag{18}$$

where $F(V_{\mathrm{rain}}(t))$ is the probability distribution of rainfall intensity.

2) Failure Rate Models of Transformers

A large proportion of distribution transformer faults are insulation accidents resulting from dampness. The main causes are as follows: a) Owing to high air humidity during hurricanes, moisture in the air enters insulations along the connecting caps; b) Rain and damp air enter transformers causing the insulating materials to get wet.

Critical rainfall intensity of insulating oil discharging and oil-impregnated paper breakdown can be expressed as:

$$\begin{cases} A_{\varsigma 1}=\left\{\left[\dfrac{W_1\pi}{a}_1 T\left(\dfrac{P_0}{P}\right)^{n_1}\right]^2-b_1\right\}^{\frac{1}{0.949}} \\ A_{\varsigma 2}=\left\{\ln\left[\dfrac{W_2\pi}{a}_2 T\left(\dfrac{P_0}{P}\right)^{n_2}\right]^2-b_2\right\}^{\frac{1}{1.323}} \end{cases} \tag{19}$$

where W_1 is the moisture content of transformer insulating oils; W_2 is the moisture content of transformer oil-impregnated paper; T is the hurricane duration; and a_1, a_2, b_1, b_2, n_1 and n_2 are all constant coefficients with the values of 0.0018, 0.591, 0, 1, 1.023 and 1.942.

The probability of insulating oil discharge is:

$$P_{\mathrm{t1}}=1-\int_0^{A_{\varsigma 1}} F(V_{\mathrm{rain}}(t))\mathrm{d}V_{\mathrm{rain}}(t) \tag{20}$$

The probability of oil-impregnated paper breakdown is:

$$P_{\mathrm{t2}}=1-\int_0^{A_{\varsigma 2}} F(V_{\mathrm{rain}}(t))\mathrm{d}V_{\mathrm{rain}}(t) \tag{21}$$

Therefore, the total failure rate of distribution transformers is:

$$P_{\mathrm{t}}=P_{\mathrm{t1}}+P_{\mathrm{t2}}-P_{\mathrm{t1}}P_{\mathrm{t2}} \tag{22}$$

D. Comprehensive Power Outage Rates of DN Loads

Considering DN topologies and failure rates of all components in DNs caused by hurricanes including the poles/towers, overhead lines, insulators and transformers, the total failure rate of the i^{th} load at moment t can be expressed as:

$$P_{\Sigma}(t)=1-\prod_{\tau\in[0,t]}(1-P_{\mathrm{r}}(\tau))(1-P_{\mathrm{l}}(\tau))+P_{\mathrm{i}}(t)+P_{\mathrm{t}}(t) \tag{23}$$

IV. Emergency Power Supply Capability of Multiple EPSVs

Emergency power supply capabilities of multiple EPSVs include the maximum discharging power and electric quantity at the beginning of each dispatching period during restoration, and multiple EPSVs show different emergency power supply capabilities under extreme disasters, such as hurricanes. For example, capabilities of electric EPSVs are determined by their powers and capacities of battery energy storage systems (BESSs), of hydrogen fuel cell EPSVs are determined by their powers of hydrogen energy storage systems (HESSs). The above differences are caused by the limited power energy stored in BESSs, but hydrogen can be replenished to HESSs locally during restoration of hurricanes.

A. Electric EPSVs

As emergency power supply sources, the capabilities of electric EPSVs in restoring outage loads under hurricanes are determined by their maximum charging/discharging power, state of charge (SoC) and mobility.

Due to the limited powers and SoCs, power supply of the i^{th} load can be maintained by the j^{th} electric EPSV based on constraints in (24).

$$\begin{cases} x_{\text{ESS}}^{i,j}(t) = 1 \\ \overline{P}_{\text{ESS}}^{j} \geq P^{i}(t) \\ E_{\text{ESS}}^{j}(t) \geq P^{i}(t)\Delta t \end{cases} \tag{24}$$

where $x_{\text{ESS}}^{i,j}(t)$ is the state whether the j^{th} electric EPSV is transported to the i^{th} load at the moment t, if $x_{\text{ESS}}^{i,j}(t)$ equals to 1, the EPSV stands by the load at moment t, as a main cause of EPSVs in transport at the beginning of dispatching periods, the congestion degree of transportation networks after hurricanes can be taken into consideration; $\overline{P}_{\text{ESS}}^{j}$ shows the maximum charging/discharging power of the j^{th} electric EPSV, which is set to 40 kW in this paper; $E_{\text{ESS}}^{j}(t)$ represents the SoC of the j^{th} BESS at moment t; $P^{i}(t)$ is the power demand of the i^{th} load at moment t; and Δt represents the duration of a dispatching period, which is 1 h in this paper. Note the power demand of loads during a dispatching period is assumed as invariable, and EPSVs are considered as emergency sources maintaining point-to-point power supply without being connected to DNs.

Considering the consumption of time and energy during the transportation of electric EPSVs, SoCs of BESSs are correlated with transportation states and power supply states.

$$E_{\text{ESS}}^{j}(t) = \overline{E}_{\text{ESS}}^{j} - \int_{0}^{t} \gamma_{\text{ESS}}^{j}(\tau)\mathrm{d}\tau \tag{25}$$

where $E_{\text{ESS}}^{j}(t)$ represents the SoC of the j^{th} BESS at moment t; $\overline{E}_{\text{ESS}}^{j}$ is the initial SoC of the j^{th} BESS at the beginning of the restoration period after hurricanes which is 250 kWh without consideration of uncertainty; $\gamma_{\text{ESS}}^{j}(\tau)$ is the power consumption during the dispatching period from τ, which can be further expressed as:

$$\gamma_{\text{ESS}}^{j}(\tau) = \begin{cases} D_{\text{ESS}}^{j}(\tau) \times E_{\text{d}} & \text{if } \max\limits_{i\in[1,m]}(x_{\text{ESS}}^{i,j}(\tau)) = 0 \\ 0 & \text{if } \max\limits_{i\in[1,m]}(x_{\text{ESS}}^{i,j}(\tau)) > 0 \\ & \&E_{\text{ESS}}^{j}(\tau) < P^{i}(\tau) \\ P^{i}(\tau) & \text{otherwise} \end{cases} \tag{26}$$

where $D_{\text{ESS}}^{j}(\tau)$ shows the transporting distance of the j^{th} electric EPSV during the dispatching period from τ; E_{d} represents per-kilometer energy consumption of EPSVs, which is 0.2 kWh in this paper; m is the amount of load nodes in DNs. Note during a dispatching period, the transportation state and power supply state of an EPSV are invariable, i.e., if the location of an EPSV must be changed, the EPSV will certainly fail to participate in power supply in the next dispatching period for transportation.

B. Hydrogen Fuel Cell EPSVs

Different from electric EPSVs, capabilities of restoring critical loads of hydrogen fuel cell EPSVs are determined by maximum charging/discharging powers of HESSs, for hydrogen can be replenished to HESSs locally during the restoration of hurricanes, where the amount and locations of hydrogen fueling stations are critical factors.

Due to the limited powers and limitless SoCs, power supply of the i^{th} load can be maintained by the j^{th} hydrogen fuel cell EPSV based on constraints in (27).

$$\begin{cases} x_{\text{HSS}}^{i,j}(t) = 1 \\ \overline{P}_{\text{HSS}}^{j} \geq P^{i}(t) \\ E_{\text{HSS}}^{j}(t) \geq P^{i}(t)\Delta t \end{cases} \tag{27}$$

where $x_{\text{HSS}}^{i,j}(t)$ is the state whether the j^{th} hydrogen fuel cell EPSV is transported to the i^{th} load at moment t, which is the same as $x_{\text{ESS}}^{i,j}(t)$; $\overline{P}_{\text{HSS}}^{j}$ shows maximum charging/discharging power of the j^{th} hydrogen fuel cell EPSV, which is set to 100 kW in this paper; $E_{\text{HSS}}^{j}(t)$ represents the SoC of the j^{th} HESSs at moment t. Note local hydrogen is assumed abundant at hydrogen fueling stations.

Moreover, transportation characteristics are the same between electric EPSVs and hydrogen fuel cell EPSVs based on their mobility, which are mainly presented as time and energy consumption.

$$E_{\text{HSS}}^{j}(t) = \overline{E}_{\text{HSS}}^{j} - \int_{0}^{t} \gamma_{\text{HSS}}^{j}(\tau)\mathrm{d}\tau \tag{28}$$

where $E_{\text{HSS}}^{j}(t)$ represents the SoC of the j^{th} HESS at moment t; $\overline{E}_{\text{HSS}}^{j}$ is the initial SoC of the j^{th} HESS at the beginning of the restoration period after hurricanes which is 500 kWh without consideration of uncertainty; $\gamma_{\text{HSS}}^{j}(\tau)$ is power consumption during the dispatching period from τ, which can be further expressed as:

$$\gamma_{\text{HSS}}^{j}(\tau) = \begin{cases} D_{\text{HSS}}^{j}(\tau) \times E_{\text{d}} & \text{if } \max\limits_{i\in[1,m]}(x_{\text{HSS}}^{i,j}(\tau)) = 0 \\ & \&y_{\text{HSS}}^{j}(\tau) = 0 \\ -\overline{P}_{\text{HSS}}^{j} & \text{if } y_{\text{HSS}}^{j}(\tau) = 1 \\ 0 & \text{if } \max\limits_{i\in[1,m]}(x_{\text{HSS}}^{i,j}(\tau)) > 0 \\ & \&E_{\text{HSS}}^{j}(\tau) < P^{i}(\tau) \\ P^{i}(\tau) & \text{otherwise} \end{cases} \tag{29}$$

where $D_{\text{HSS}}^{j}(\tau)$ shows the transporting distance of the j^{th} HESS during the dispatching period from τ; $y_{\text{HSS}}^{j}(\tau)$ is whether the j^{th} HESS is transported to the hydrogen fueling station at the moment t, if $y_{\text{HSS}}^{j}(\tau)$ equals to 1, the EPSV stands by the hydrogen fueling station.

V. Allocation Strategy of Multiple EPSVs Balancing Resilience and Economics

On the basis of mobility characteristics, EPSVs can be used to restore critical loads after hurricanes, however, EPSVs are usually idle under normal states. Therefore, it is necessary

to propose an allocation strategy of EPSVs to balance the resilience and economics of DNs optimally.

A. Multi-Objective Optimization Allocation Strategy of EPSVs

In the restoration period of hurricanes, EPSVs are used to restore critical loads and enhance resilience of DNs with a huge investment. Therefore, a multi-objective optimization model balancing the resilience and economics of DNs is proposed as follows.

$$\min(F_{\mathrm{C}}, F_{\mathrm{E}}) \tag{30}$$

where F_{C} and F_{E} are the resilience and economic indexes of DNs based on multiple EPSVs, respectively. Note to deal with various time scales of the resilience index and the economic index, all typical hurricane scenarios are considered to transform the time scale of the resilience index into the whole planning period, where typical hurricane scenarios are generated by the proposed statistic-mechanism failure rate model of DNs.

1) Sub-objective of Resilience

A resilience-oriented allocation strategy is usually used to seek minimum outage power loss under all hurricanes during the whole planning period.

$$\min F_{\mathrm{C}} = \gamma \int_0^{t_{\mathrm{total}}} \sum_{i=1}^{m} (c_{\mathrm{i}} P_{\mathrm{i}}(t) P_{\Sigma}(t)(1 - n_{\mathrm{i}}(t))) \mathrm{d}t \tag{31}$$

where γ is the frequency of hurricanes during the planning period; t_{total} represents the restoration period, which is 8 h in this paper; c_{i} is the outage power loss of the i^{th} load, where $c_1, c_2, \cdots, c_m$ are the prioritized outage power loss of loads; $P_{\mathrm{i}}(t)$ is the outage power for the i^{th} load at moment t; and $n_{\mathrm{i}}(t)$ is the power supply state of the i^{th} load at moment t by allocating EPSVs, which is valued as 1 when (24) or (27) is satisfied, and it is related to the congestion degree of transportation networks after hurricanes.

2) Sub-objective of Economics

An economics-oriented allocation strategy of EPSVs is usually proposed for the minimum investment cost, maintenance cost and reliability improvement. Economics sub-objective can be expressed as:

$$\begin{aligned} \min F_{\mathrm{E}} = {} & M_{\mathrm{ESS}} \left(\frac{n}{N} C_{\mathrm{f}}^{\mathrm{ESS}} + \frac{T_{\mathrm{p}}}{24} C_{\mathrm{m}}^{\mathrm{ESS}} \overline{P}_{\mathrm{ESS}} T_{\mathrm{ESS}} \right) \\ & + M_{\mathrm{HSS}} \left(\frac{n}{N} C_{\mathrm{f}}^{\mathrm{HSS}} + \frac{T_{\mathrm{p}}}{24} C_{\mathrm{m}}^{\mathrm{HSS}} \overline{P}_{\mathrm{HSS}} T_{\mathrm{HSS}} \right) \\ & - \frac{T_{\mathrm{p}}}{8760} \bar{c} E_{\mathrm{ENS}} \end{aligned} \tag{32}$$

where M_{ESS} and M_{HSS} are the amount of electric EPSVs and hydrogen fuel cell EPSVs respectively; n is the frequency of charging/discharging during the simulation; N is the life cycle of EPSVs, which is set to 4000; $C_{\mathrm{f}}^{\mathrm{ESS}}$ and $C_{\mathrm{f}}^{\mathrm{HSS}}$ are the unit investment cost of electric EPSVs and hydrogen fuel cell EPSVs respectively, which are 3 million CNY/set and 5 million CNY/set; T_{p} indicates the planning period of EPSVs; $C_{\mathrm{m}}^{\mathrm{ESS}}$ and $C_{\mathrm{m}}^{\mathrm{HSS}}$ represents the unit maintenance cost of electric EPSVs and hydrogen fuel cell EPSVs respectively, which are 0.12CNY/kW/day and 0.2CNY/kW/day; T_{ESS} and T_{HSS} are the charging/discharging time of electric EPSVs and hydrogen fuel cell EPSVs with maximum charging/discharging power; $\bar{c}$ is the average outage power loss of loads under normal states, which is 1 CNY/kW; and E_{ENS} represents the expected value of energy not supplied in a year [30].

3) Constraints

During the restoration period considering the dispatching of electric EPSVs and hydrogen fuel cell EPSVs, constraints of power supply states, power supply capabilities and uniqueness of EPSVs must be obeyed strictly.

a) Power supply state. The state constraint of the j^{th} EPSV at moment t are shown in (24) and (27), which is determined by transportation states, powers and capacities for electric EPSVs, but only correlated with transportation states and powers for hydrogen fuel cell EPSVs.

b) Power supply capability. Owing to the limited power energy of BESSs and HESSs, the SoCs of electric EPSVs and hydrogen fuel cell EPSVs are required to satisfy the constraint in (26) considering whether the j^{th} EPSV is in transport, idle at the i^{th} load, or maintaining the power supply of the i^{th} load during the dispatching period from τ.

c) Uniqueness of EPSVs. At moment t, only one EPSV, at most, is utilized to maintain power supply of the i^{th} load, so the following constraint must be met.

$$\sum_{j=1}^{M_{\mathrm{ESS}}} x_{\mathrm{ESS}}^{i,j}(t) + \sum_{j=1}^{M_{\mathrm{HSS}}} x_{\mathrm{HSS}}^{i,j}(t) \le 1 \tag{33}$$

B. Equilibrium Model Between Resilience and Economics Based on Nash Equilibrium

The weighted sum scalarization technique and ε-constrained method are not suitable for transforming the above multi-objective problem of multiple ESSs allocation strategy into a single-objective problem for the HILP characteristics [31], [32], because it cannot deal with the huge diversity of dimensions, magnitudes and probabilities between multiple objectives, which influence uniformity of frontier a lot. Therefore, a bargaining model is presented to achieve a Nash equilibrium in the pre-hurricane allocation through approaching the Pareto's optimal frontier by choosing resilience and economics as two players.

The resilience F_{C} and economics F_{E} of DNs are usually opposite stakeholders; they are usually regarded as two players in the bargaining process. To obtain an optimal allocation of multiple EPSVs, an equilibrium model is established with the objective of:

$$\max_{x \in X} (d_1 - F_{\mathrm{C}})(d_2 - F_{\mathrm{E}}) \tag{34}$$

where d_1 and d_2 are the critical values of the resilience sub-objective and economics sub-objective.

Note the existence of Nash equilibrium of a finite strategy game was proved (Nash, 1950), and if the Nash equilibrium point lies on the Pareto frontier, the multi-objective optimization problem gains an optimal solution, otherwise, a Pareto optimal solution approaching to the Nash equilibrium point is chosen as the optimal solution based on the theorem 8.4 in reference [33].

The Pareto optimal frontier is gradually approached through continuous bargaining, and the equilibrium solution is obtained. According to the linear transformation invariance principle, an equilibrium model is established by linear transformations to depict HILP events, such as hurricanes, and normal states, so different dimensions and magnitudes of resilience and economics can be retained. Therefore, an equilibrium allocation of EPSVs is gained on the basis of bargaining between resilience and economics through allocating multiple EPSVs.

Then, the multi-objective optimization model in (30) is solved by NSGA-II algorithm [34], so a Pareto optimal frontier is obtained, which is formed by all optimal allocation results of multiple EPSVs. Since the multi-objective optimization is converted into a single-objective one as shown in (34), GA method is used to gain an equilibrium point on the Pareto optimal frontier, the equilibrium point represents the equilibrium allocation of multiple EPSVs balancing the resilience and economics of DNs. Finally, the optimal allocation of multiple EPSVs is gained containing amounts and locations of electric EPSVs and hydrogen fuel cell EPSVs.

VI. Case Study

A. Simulation Background

An IEEE 33-node DN in hurricane-prone areas is chosen to verify the proposed allocation strategy with a planning period of 10 years. The following two aspects will be emphasized; one is the accuracy of failure rate models of DNs under hurricanes considering strong winds and rainfall, the other is the effectiveness of the equilibrium allocation strategy of EPSVs based on Nash equilibrium method.

As shown in Fig. 2, a coordinate system is set up, and east is taken as the positive direction of the x-axis, the north is taken as the positive direction of the y-axis. It is assumed that geographical connections between adjacent loads are the same as electrical distances, and the type of overhead lines in the DNs is LGJ-240/30 [35]. Electrical distances and temporal curve of loads of the simulated DN are shown as Table I and Fig. 3, and loads are divided into two types according to their importance under hurricanes: nodes in red are critical loads with unit outage power loss $c_1 = 1000$ CNY/kW, and others are normal loads with unit outage power loss $c_2 = 100$ CNY/kW. The reliability of power supply of the simulated DN achieves 99.999%, and a hydrogen fueling station is located at Node 8. It is assumed a hurricane occurs 10 times per year in the range of DNs at any time during a day, and the hurricane is centered at (200, −80) with a radius of 30 km, the speed of the hurricane is 12 km/h to the north and 8 km/h to the west.

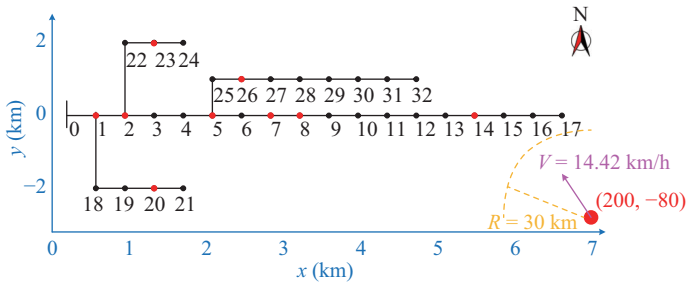

Fig. 2. Topology of the IEEE 33-node DN in hurricane-prone areas.

TABLE I
Parameters of the Simulated IEEE-33 Node DN

Initial node	End node	Distance (km)	Maximum load power (kW)	Importance degree
0	1	0.4	100	2
1	2	0.4	90	1
2	3	0.4	120	2
3	4	0.4	60	2
4	5	0.4	60	2
5	6	0.4	200	2
6	7	0.4	200	1
7	8	0.4	60	1
8	9	0.4	60	2
9	10	0.4	45	2
10	11	0.4	60	2
11	12	0.4	60	2
12	13	0.4	120	2
13	14	0.4	60	1
14	15	0.4	60	2
15	16	0.4	60	2
16	17	0.4	90	2
1	18	2	90	2
18	19	0.4	90	2
19	20	0.4	90	1
20	21	0.4	90	2
2	22	2	90	2
22	23	0.4	120	2
23	24	0.4	120	2
5	25	1	60	2
25	26	0.4	60	2
26	27	0.4	60	2
27	28	0.4	120	2
28	29	0.4	200	2
29	30	0.4	150	2
30	31	0.4	100	2
31	32	0.4	60	2

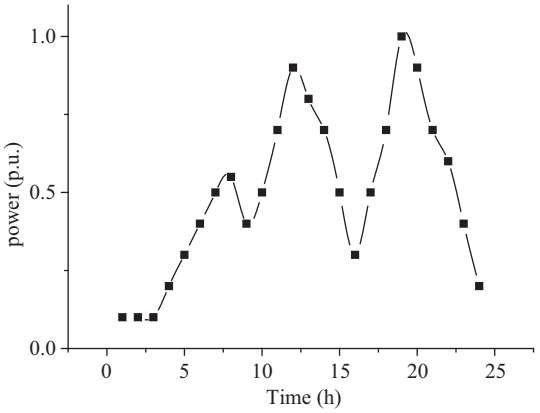

Fig. 3. Temporal curve of resident loads in the simulated DN.

B. DN Failure Rate Models Under Hurricanes

To achieve an optimal pre-hurricane allocation, it is necessary to model meteorological data and measure line/component failure rates of DNs under hurricanes accurately.

Through the analysis of hurricane historical data on the website of China meteorological administration (CMA) [36], temporal variations of hurricane intensity are shown in Fig. 4(a) and Fig. 4(b), note that each point on the curve is obtained by the mean value of the Gaussian distribution, which is the

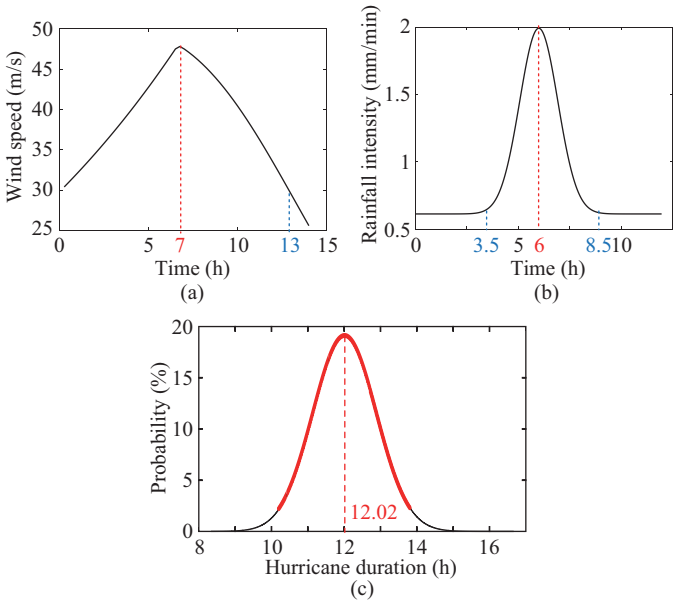

Fig. 4. Temporal distributions of hurricane intensity and duration. (a) Temporal distribution of wind speed. (b) Temporal distribution of rainfall intensity. (c) PDF of hurricane duration.

PDF fitted by hurricane intensity data at that moment. The instantaneous values of wind speed and rainfall intensity are characterized by the 95% conditional confidence interval of the fitted Gaussian distribution, where the average fitting error of wind speed and rainfall intensity during the whole hurricane duration are 7.38% and 6.57%, respectively. A regression analysis of hurricane duration based on historical data has been adopted, and the PDF is shown as Fig. 4(c). In addition, hurricane duration is found to be Gaussian with a mean of 12.02h and a variance of 2.09, so the mean value can be taken as the predicted hurricane duration, i.e., $t_{\text{total}} = 12.02$ h.

Based on the hurricane intensity and duration, the failure rate of DNs can be obtained under strong winds and rainfall. The instantaneous wind speed of hurricanes leads to wind loads on poles, towers and overhead lines of DNs resulting in fallen poles/towers and broken overhead lines. However, as the distances between adjacent poles and towers of DNs are short and arcs of overhead lines are small, the probability of fallen poles/towers is greater than of broken overhead lines. In addition, heavy rainfall caused by hurricanes result in failures of insulators and transformers submerged in water. The failure rate of transformer insulation due to substation flooding is greater. According to the failure rate models shown in (13), (16), (18), and (22), total failure rates of DNs under hurricanes are presented in Table II. It can be calculated the failure rate caused by rainfall accounts for 19.37% of the total failure rate of DNs, which cannot be ignored. Therefore, during evaluation of the failure rate of DNs, the proposed failure rate models show great advantages.

C. Optimal Allocation Results of EPSVs

To verify superiority of the proposed pre-hurricane allocation strategy based on multiple EPSVs, simulation studies are conducted to evaluate allocation considering concurrent disasters, equilibrium allocation considering resilience and economics, sensitivity of EPSV allocation strategy, and superiority of allocating multiple EPSVs jointly.

TABLE II
FAILURE RATES OF A NODE UNDER HURRICANES

Component	Failure rate (%)
Pole/Tower	3.65
Overhead line	1.27
Total (under winds)	4.87
Insulator	0.01
Transformer	1.16
Total (under rainfalls)	1.17
Total	6.04

1) Resilience-oriented Allocation of EPSVs Considering Concurrent Disasters

To verify the proposed failure rate models considering strong winds and rainfall in Section III and Section IV, simulation cases are organized based on different failure rate models as follows:

Case 1-1: Considering the impact of wind speed on failure rates of DNs individually, pre-hurricane allocation results of EPSVs are optimized to improve resilience of DNs;

Case 1-2: Considering the impact of wind speed, rainfall intensity and hurricane duration on failure rates of DNs, pre-hurricane allocation results of EPSVs are optimized to improve resilience of DNs.

By solving allocation strategy models of EPSVs, allocation results and outage power loss are shown in Table III. It is verified that considering wind speed individually in *Case 1-1*, 25 electric EPSVs and 2 hydrogen fuel cell EPSVs are needed in the simulated DN, and resilience measured by outage power loss is 0.4 million CNY under every hurricane. If wind speed, rainfall intensity and hurricane duration are considered jointly as *Case 1-2*, the amount of electric EPSVs increases to 33, all loads can be restored during every hurricane. A decrease of 40.49 million CNY in outage power loss is achieved by increasing the 8 EPSVs, and all critical loads are restored under hurricanes. Therefore, the proposed failure rate models of DNs under hurricanes show superiority in enhancing the resilience of DNs by pre-hurricane allocation considering wind speed, rainfall intensity and hurricane duration jointly.

TABLE III
ALLOCATION RESULTS BASED ON DIFFERENT FAILURE RATE MODELS

Case	Amount of electric EPSVs (set)	Amount of hydrogen fuel cell EPSVs (set)	F_{C} (Million CNY)
1-1	25	2	40.49
1-2	33	2	0

2) EPSV Allocation Balancing Resilience and Economics

To verify the overall advantages of the proposed Nash equilibrium model on balancing resilience and economics in (34), based on the same failure rate models of DNs as *Case 1-2*, simulation cases of allocation electric EPSVs and hydrogen fuel cell EPSVs solved by different methods are organized as follows:

Case 2-1: *Case 2-1* is the same as *Case 1-2*, which is resilience-oriented.

Case 2-2: Equilibrium of the resilience and economics of DNs based on the entropy weight method, weights of the resilience sub-objective and economics sub-objective are set to 2/73 and 71/73 considering the occurrence probabilities of hurricanes and normal states. The objective can be shown as $\min_{x\in X}\left(\frac{2}{73}F_{\mathrm{C}}+\frac{71}{73}F_{\mathrm{E}}\right)$;

Case 2-3: Equilibrium of the resilience and economics of DNs based on the entropy weight method, weights of the resilience sub-objective and economics sub-objective are set to 6/25 and 19/25 [37]. The objective can be shown as $\min_{x\in X}\left(\frac{6}{25}F_{\mathrm{C}}+\frac{19}{25}F_{\mathrm{E}}\right)$;

Case 2-4: Equilibrium of the resilience and economics of DNs based on the Nash equilibrium method as shown in (34). Critical values of the resilience sub-objective and economics sub-objective are set to $d_1 = 7270$ million and $d_2 = 50$ million. It should be noted that d_1 depends on the outage costs of all loads, and d_2 is maximum investment cost of purchasing multiple EPSVs.

Allocation results of EPSVs, resilience and economics are shown in Table IV. As shown in *Case 2-1*, all loads can be restored with 33 electric EPSVs and 2 hydrogen fuel cell EPSVs. The investment cost, maintenance cost and reliability improvement are 109.72 million CNY. Different from *Case 2-1*, the equilibrium of resilience and economics of DNs is applied in *Case 2-2* and *Case 2-3* with different weights of entropy weight method. Because of the high magnitude of hurricane impact, the resilience index constitutes the main factor of the weighted objective. Allocation results verge on a resilience-oriented allocation with an investment boundary 50 million CNY, but there are still 3877.9 million CNY power outage losses in *Case 2-2* weighting objectives according to occurrence probabilities of hurricanes and normal states, and 3852.47 million CNY power outage losses in *Case 2-3* by increasing the weight of resilience of DNs. However, comparing *Case 2-4* with *Case 2-2* and *Case 2-3*, only 16.88 million CNY of power outage losses is increased by decreasing more than 50% investment. That is, in *Case 2-4*, the Nash equilibrium method is adopted and an equilibrium allocation result of 3 electric EPSVs and 3 hydrogen fuel cell EPSVs is conducted.

TABLE IV
ALLOCATION RESULTS BASED ON DIFFERENT EQUILIBRIUM MODELS

Case	Amount (set)		Equilibrium benefit (million CNY)		(d_1-F_{C}) (d_2-F_{E}) (million ^{2})
	Electric EPSVs	Hydrogen fuel cell EPSVs	F_{C}	F_{E}	
2-1	33	2	0	109.72	–
2-2	4	7	3877.9	47.58	8209.7
2-3	8	5	3852.47	49.5	1695.65
2-4	3	3	5553	24.27	44178

3) Sensitivity Analysis of EPSV Equilibrium Allocation

To further verify the sensitivity of EPSVs allocation results solved by the proposed equilibrium allocation strategy, Fig. 5 presents the gradient between resilience and economics, where units of resilience and economics are billion CNY and million CNY, respectively. It is obvious that magnitudes of the above two indexes vary a lot, so the traditional entropy weight method is unavailable to obtain an equilibrium allocation of multiple EPSVs.

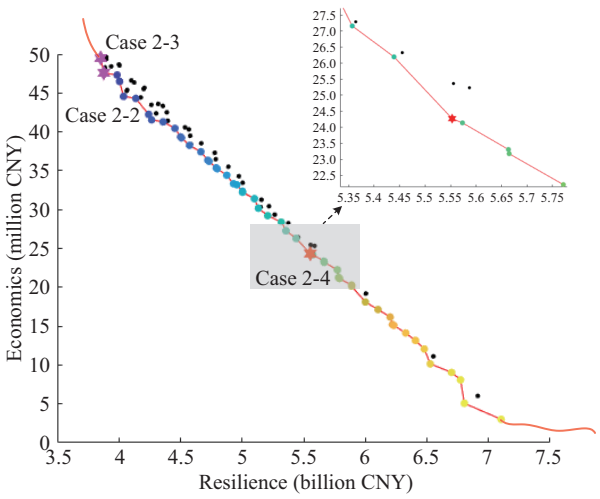

Fig. 5. Pareto curve of multi-objective optimization and allocation results.

As the investment of allocation results in *Case 2-1* exceed the boundary of investment, the feasible region in Fig. 5 cannot present the above results. Optimal allocation results in *Case 2-2* and *Case 2-3* are distributed in the terminal of the curve, which lead to an imbalance between resilience and economics of DNs. As for *Case 2-4*, optimal allocation results of the proposed equilibrium method is distributed in the middle of the Pareto curve and adjacent to the inflection point of the curve, which shows the variation rate of resilience becomes slow from the point by increasing investment.

To analyze the equilibrium allocation results solved by entropy weight method and Nash equilibrium method, Table V is presented to compare the effects of results in *Case 2-3* and *Case 2-4*. At the equilibrium point gained by *Case 2-3*, a 50.94 million CNY outage power loss is reduced by increasing 1 million CNY investment, the variation rate is similar when reducing the amount of multiple EPSVs. At the equilibrium point obtained by *Case 2-4*, a 106.2 million CNY outage power loss is increased by reducing 1 million CNY investment, which is more than 1.61 times of *Case 2-3*. The variation rate is approximate to *Case 2-3* when increasing the amount of multiple EPSVs. That means the gradient of power outage loss is reduced slowly by reinvesting emergency power supply sources but increased rapidly by cutting down investment. Therefore, the equilibrium result of *Case 2-4* is better than *Case 2-3*, so the superiority of the proposed equilibrium allocation strategy based on the Nash equilibrium model is proved.

4) Superiority of Allocating Multiple EPSVs Jointly

To verify the superiority of allocating multiple EPSVs jointly, based on the same failure rate models of DNs as *Case 1-2*, simulation cases of allocating different types of EPSVs balancing resilience and economics by Nash equilibrium method are organized as follows:

Case 3-1: Only electric EPSVs are allocated to improve the resilience and economics of DNs;

Case 3-2: Only hydrogen fuel cell EPSVs are allocated to

TABLE V
SENSITIVITY OF OPTIMAL ALLOCATION RESULTS

Objectives	Case 2-3		Case 2-4	
Variation of economics (million CNY)	−1	1	−1	1
Variation of resilience (million CNY)	66.02	−50.94	106.2	−66.85

TABLE VI
ALLOCATION RESULTS BASED ON DIFFERENT TYPES OF EPSVS

Case	Amount (set)		Equilibrium benefit (million CNY)		$(d_1 - F_C)$ $(d_2 - F_E)$ (Million CNY^2)
	Electric EPSVs	Hydrogen fuel cell EPSVs	F_C	F_E	
3-1	9	0	5757	27.16	34562.43
3-2	0	4	5735.63	23.36	40264.87
3-3	3	3	5553	24.27	44178
3-4	4	3	5604.68	27.29	37819.42

improve the resilience and economics of DNs;

Case 3-3: *Case 3-3* is the same as *Case 2-4*, which aims at improving the resilience and economics by allocating electric EPSVs and hydrogen fuel cell EPSVs jointly.

Case 3-4: *Case 3-4* is similar to *Case 3-3*, but the hydrogen fueling station is located at Node 14.

Table I shows optimal allocation of EPSVs in *Case 3-1* to *Case 3-4*, which is presented to capture the advantage of utilizing both electric EPSVs and hydrogen fuel cell EPSVs jointly, restoring outage loads after hurricanes. In *Case 3-1*, 9 electric EPSVs are allocated to maintain continuous power supply of critical loads in the simulated DN with an investment of 27.16 million CNY, but there are still 5757 million CNY power outage losses during the whole planning period. However, only 4 hydrogen fuel cell EPSVs are allocated in *Case 3-2*, which lead to a similar resilience index to *Case 3-1*. The main reason is both the powers and capacities of ESSs are limited, but capacities of HESSs are limitless for the abundant hydrogen locally. So, the investment is cut down to 23.36 million CNY, and the objective calculated by (34) shows better. Comparing the above cases allocating single type of EPSVs with *Case 3-3*, which adopts electric EPSVs and hydrogen fuel cell EPSVs in restoring outage loads after hurricanes, 182.63 million CNY of outage power loss is reduced with low investment, the maximum objective is gained through allocating 3 electric EPSVs and 3 hydrogen fuel cell EPSVs. Comparing *Case 3-1*, *Case 3-2* with *Case 3-4*, advantages of allocating electric EPSVs and hydrogen fuel cell EPSVs jointly, cannot be reflected without proper location of the hydrogen fueling station. Moreover, the importance of locations of hydrogen fueling stations is further verified comparing *Case 3-3*and *Case 3-4*, so more electric EPSVs are required if the hydrogen fueling station is far away from critical loads, but less power is restored with higher investment.

To further portray the strength of multiple EPSVs after hurricanes, a restoration period lasting 8 hours is conducted from 8:00 a.m. As shown in Fig. 6, temporal restored power and output power of multiple EPSVs are accessed. In *Case 3-1*, the

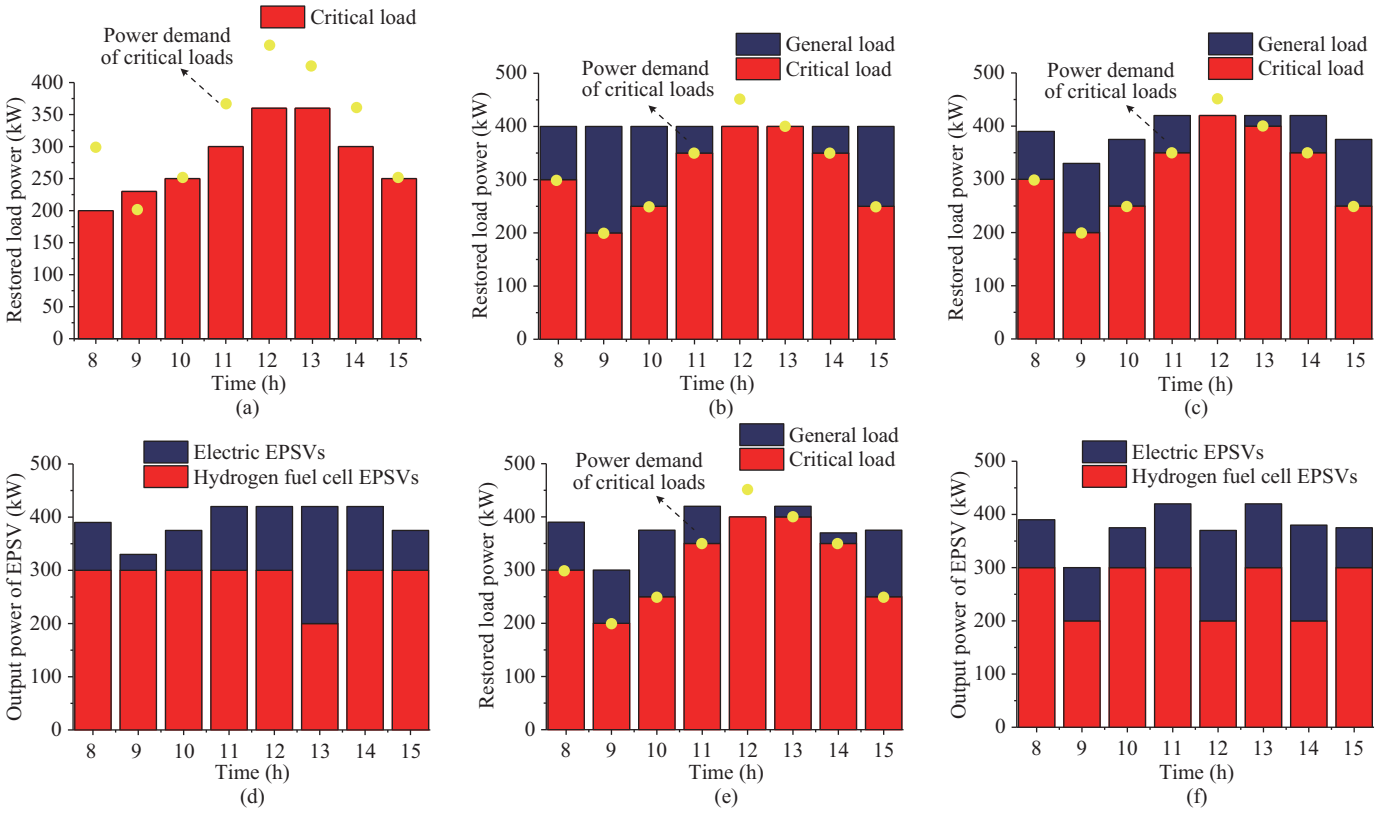

Fig. 6. Restoration strategy after hurricanes by allocating different of EPSVs. (a) Temporal restored load powers in *Case 3-1*. (b) Temporal restored load powers in *Case 3-2*. (c) Temporal restored load powers in *Case 3-3*. (d) Temporal output powers of multiple EPSVs in *Case 3-3*. (e) Temporal restored load powers in *Case 3-4*. (f) Temporal output powers of multiple EPSVs in *Case 3-4*.

maximum output power of all 9 electric EPSVs are 360 kW, which cannot meet the required power of critical loads in peak durations, such as 12:00–13:00, and total restored load for 8 hours is 2250 kWh. In *Case 3-2*, the maximum output power of all 4 EPSVs with HSSSs are 400 kW, which can satisfy most required power of critical loads during the restoration period. By utilizing the maximum output power of hydrogen fuel cell EPSVs, total restored load for 8 hours approaches to 3200 kWh. In *Case 3-3*, the maximum output power of 3 electric EPSVs and 3 hydrogen fuel cell EPSVs is 420 kW, which is even higher than *Case 3-2*. Although the total restored load for 8 hours is 50 kWh less than *Case 3-2*, the weighted restored load is greater, because more critical loads can be restored in peak durations based on the larger output powers in *Case 3-3* with a smaller electric quantity. Therefore, the optimal coordination of powers and capacities during a temporal restoration period is gained by allocating electric EPSVs and hydrogen fuel cell EPSVs jointly, which leads to the optimal restoration effect in both time and space. Optimal locations of *Case 3-3* and *Case 3-4* are shown in Tables VII and VIII, in *Case 3-3*, EPSV 1 to EPSV 3 are electric EPSVs, others are hydrogen fuel cell EPSVs; but in in *Case 3-4*, EPSV 1 to EPSV 4 are electric EPSVs. Comparing *Case 3-3* and *Case 3-4*, less loads are restored in *Case 3-4*for EPSV 6 is being transported to the hydrogen fueling station far away from critical loads at 9:00 and 12:00, and EPSV 7 is replenishing hydrogen at the hydrogen fueling station at 14:00, so it is confirmed that dispatching routes of multiple EPSVs and locations of hydrogen fueling stations impact the restoration effect a lot.

TABLE VII
OPTIMAL LOCATIONS OF MULTIPLE EPSVS IN *Case 3-3*

Time (h)	EPSV 1	EPSV 2	EPSV 3	EPSV 4	EPSV 5	EPSV 6
8	2	20	14	8	6	7
9	2	20	14	8	6	7
10	2	20	14	8	6	7
11	2	20	14	8	5	7
12	5	14	20	2	7	8
13	5	14	20	2	7	8
14	20	14	2	8	7	8
15	20	14	2	8	7	8

TABLE VIII
OPTIMAL LOCATIONS OF MULTIPLE EPSVS IN *Case 3-4*

Time (h)	EPSV 1	EPSV 2	EPSV 3	EPSV 4	EPSV 5	EPSV 6
8	2	4	7	8	6	20
9	2	20	7	8	6	–
10	2	4	7	8	6	20
11	2	4	7	8	5	20
12	5	14	8	2	7	–
13	5	4	8	2	7	14
14	20	4	8	8	7	14
15	20	2	8	8	7	14

VII. CONCLUSION

This paper focused on a novel pre-hurricane equilibrium allocation strategy of electric EPSVs and hydrogen fuel cell EPSVs being proposed considering the balance of the resilience and economics of DNs, the main conclusions of this paper are summarized as follows:

1) The accuracy of line/component failure rate models of DNs is improved by CVaR method considering strong wind speed, consequent rainfall, and hurricane duration jointly. The proposed failure rate models of DNs are more accurate, which account for 19.37% of total failure rate.

2) The Nash equilibrium model for balancing the resilience and economics can enhance resilience of DNs while limiting investment. Compared with traditional portrayed weight method, the proposed method increases only 16.88 million CNY of power outage loss by decreasing more than 50% investment.

3) By allocating electric EPSVs and hydrogen fuel cell EPSVs jointly, coordination of powers and capacities are attained during the restoration period after hurricanes, which makes full use of multiple EPSVs' advantages. Compared with allocating a single type of EPSVs, the proposed method can obtain less outage power losses by utilizing 50 kWh less electric quantity during a restoration period after hurricanes.

REFERENCES

[1] N. Safaei, D. Banjevic, and A. K. S. Jardine, "Workforce planning for power restoration: an integrated simulation-optimization approach," *IEEE Transactions on Power Systems*, vol. 27, no. 1, pp. 442–449, Feb. 2012.

[2] A. Arab, A. Khodaei, S. K. Khator, K. Ding, V. A. Emesih, and Z. Han, "Stochastic pre-hurricane restoration planning for electric power systems infrastructure," *IEEE Transactions on Smart Grid*, vol. 6, no. 2, pp. 1046–1054, Mar. 2015.

[3] K. Itani, A. De Bernardinis, Z. Khatir, A. Jammal, and M. Oueidat, "Regenerative braking modeling, control, and simulation of a hybrid energy storage system for an electric vehicle in extreme conditions," *IEEE Transactions on Transportation Electrification*, vol. 2, no. 4, pp. 465–479, Dec. 2016.

[4] H. Khani, N. A. El-Taweel, and H. E. Z. Farag, "Supervisory scheduling of storage-based hydrogen fueling stations for transportation sector and distributed operating reserve in electricity markets," *IEEE Transactions on Industrial Informatic*s, vol. 16, no. 3, pp. 1529–1538, Mar. 2020.

[5] J. Booth, M. Drye, D. Whensley, P. McFarlane, and S. McDonald, "Future of flood resilience for electricity distribution infrastructure in Great Britain," *CIRED – Open Access Proceedings Journal*, vol. 2017, no. 1, pp. 1158–1161, Oct. 2017.

[6] M. Bessani, J. A. D. Massignan, R. Z. Fanucchi, M. H. M. Camillo, J. B. A. London, A. C. B. Delbem, and C. D. Maciel, "Probabilistic assessment of power distribution systems resilience under extreme weather," *IEEE Systems Journal*, vol. 13, no. 2, pp. 1747–1756, Jun. 2019.

[7] R. Moreno and G. Strbac, "Integrating high impact low probability events in smart distribution network security standards through CVaR optimisation," in *IET International Conference on Resilience of Transmission and Distribution Networks (RTDN) 2015*, Birmingham, 2015, pp. 1–6.

[8] C. Wang, P. Ju, S. B. Lei, Z. Y. Wang, F. Wu, and Y. H. Hou, "Markov decision process-based resilience enhancement for distribution systems: an approximate dynamic programming approach," *IEEE Transactions on Smart Grid*, vol. 11, no. 3, pp. 2498–2510, May 2020.

[9] C. Chen and B. Chen, "Modernizing distribution system restoration to achieve resiliency against extreme weather events," in *2018 IEEE Global Conference on Signal and Information Processing (GlobalSIP)*, Anaheim, CA, USA, 2018, pp. 895–896.

[10] Y. Xu, C. C. Liu, K. P. Schneider, F. K. Tuffner, and D. T. Ton, "Microgrids for service restoration to critical load in a resilient distribution system," *IEEE Transactions on Smart Grid*, vol. 9, no. 1, pp. 426–437, Jan. 2018.

[11] S. B. Lei, J. H. Wang, and Y. H. Hou, "Remote-controlled switch allocation enabling prompt restoration of distribution systems," *IEEE Transactions on Power Systems*, vol. 33, no. 3, pp. 3129–3142, May 2018.

[12] X. Wang, Z. Y. Li, M. Shahidehpour, and C. W. Jiang, "Robust line hardening strategies for improving the resilience of distribution systems with variable renewable resources," *IEEE Transactions on Sustainable Energy*, vol. 10, no. 1, pp. 386–395, Jan. 2019.

[13] Y. Wang, Y. Xu, J. X. Li, C. Li, J. H. He, J. Y. Liu, and Q. Q. Zhang, "Dynamic load restoration considering the interdependencies between power distribution systems and urban transportation systems," *CSEE Journal of Power and Energy Systems*, vol. 6, no. 4, pp. 772–781, Dec. 2020.

[14] W. Yuan, J. H. Wang, F. Qiu, C. Chen, C. Q. Kang, and B. Zeng, "Robust optimization-based resilient distribution network planning against natural disasters," *IEEE Transactions on Smart Grid*, vol. 7, no. 6, pp. 2817–2826, Nov. 2016.

[15] X. Y. Jiang, J. Chen, M. Chen, and Z. Wei, "Multi-stage dynamic post-disaster recovery strategy for distribution networks considering integrated energy and transportation networks," *CSEE Journal of Power and Energy Systems*, vol. 7, no. 2, pp. 408–420, Mar. 2021.

[16] Q. Fu, W. J. Du, H. F. Wang, B. X. Ren, and X. Y. Xiao, "Small-signal stability analysis of a VSC-MTDC system for investigating DC voltage oscillation," *IEEE Transactions on Power Systems*, vol. 36, no. 6, pp. 5081–5091, Nov. 2021.

[17] S. B. Lei, J. H. Wang, C. Chen, and Y. H. Hou, "Mobile emergency generator pre-positioning and real-time allocation for resilient response to natural disasters," *IEEE Transactions on Smart Grid*, vol. 9, no. 3, pp. 2030–2041, May 2018.

[18] M. Y. Yan, M. Shahidehpour, A. Paaso, L. X. Zhang, A. Alabdulwahab, and A. Abusorrah, "Distribution system resilience in ice storms by optimal routing of mobile devices on congested roads," *IEEE Transactions on Smart Grid*, vol. 12, no. 2, pp. 1314–1328, Mar. 2021.

[19] S. B. Lei, C. Chen, H. Zhou, and Y. H. Hou, "Routing and scheduling of mobile power sources for distribution system resilience enhancement," *IEEE Transactions on Smart Grid*, vol. 10, no. 5, pp. 5650–5662, Sep. 2019.

[20] Y. Xu, Y. Wang, J. H. He, M. Y. Su, and P. H. Ni, "Resilience-oriented distribution system restoration considering mobile emergency resource dispatch in transportation system," *IEEE Access*, vol. 7, pp. 73899–73912, Jun. 2019.

[21] F. H. Jufri, V. Widiputra, and J. Jung, "State-of-the-art review on power grid resilience to extreme weather events: definitions, frameworks, quantitative assessment methodologies, and enhancement strategies," *Applied Energy*, vol. 239, pp. 1049–1065, Apr. 2019.

[22] V. B. Venkateswaran, D. K. Saini, and M. Sharma, "Approaches for optimal planning of the energy storage units in distribution network and their impacts on system resiliency," *CSEE Journal of Power and Energy Systems*, vol. 6, no. 4, pp. 816–833, Dec. 2020.

[23] M. Nazemi, M. Moeini-Aghtaie, M. Fotuhi-Firuzabad, and P. Dehghanian, "Energy storage planning for enhanced resilience of power distribution networks against earthquakes," *IEEE Transactions on Sustainable Energy*, vol. 11, no. 2, pp. 795–806, Apr. 2020.

[24] S. L. Wen, H. Lan, Q. Fu, D. C. Yu, and L. J. Zhang, "Economic allocation for energy storage system considering wind power distribution," *IEEE Transactions on Power Systems*, vol. 30, no. 2, pp. 644–652, Mar. 2015.

[25] S. M. Mazhari, H. Monsef, and R. Romero, "A multi-objective distribution system expansion planning incorporating customer choices on reliability," *IEEE Transactions on Power Systems*, vol. 31, no. 2, pp. 1330–1340, Mar. 2016.

[26] S. W. Miu, "Reliability evaluation techniques and their applications for wind-integrated power systems considering complicated wind characteristics," Ph.D. dissertation, Department, Chongqing University, Chongqing, 2017.

[27] S. Q. Zhang, Y. F. He, J. L. Cai, and J. W. Wang, "A new method based on Monte Carlo simulation for reliability evaluation of distribution network considering the influence of typhoon," in *2018 International Conference on Power System Technology (POWERCON)*, Guangzhou, 2018, pp. 3341–3346.

[28] M. Hurkala, B. O'Halloran, H. Nikula, S. Sierla, T. Karhela, and V. Vyatkin, "Evaluation of electric grid automation under flood hazards," in *IECON 2013–9th Annual Conference of the IEEE Industrial Electronics Society*, Vienna, 2013, pp. 4380–4385.

[29] H. C. Miller, "Surface flashover of insulators," *IEEE Transactions on Electrical Insulation*, vol. 24, no. 5, pp. 765–786, Oct. 1989.

[30] Y. Ding, C. Singh, L. Goel, J. Østergaard, and P. Wang, "Short-term and medium-term reliability evaluation for power systems with high penetration of wind power," *IEEE Transactions on Sustainable Energy*, vol. 5, no. 3, pp. 896–906, Jul. 2014.

[31] S. X. Zhang, H. Z. Cheng, K. Li, N. L. Tai, D. Wang, and F. R. Li, "Multi-objective distributed generation planning in distribution network considering correlations among uncertainties," *Applied Energy*, vol. 226, pp. 743–755, Sep. 2018.

[32] Z. W. Li, S. Q. Zhao, D. X. Li, and T. T. Zhang, "Fast solving of day-ahead power system scheduling chance-constrained model based on improved ε-constrained and deterministic transform by sampling," *Proceedings of the CSEE*, vol. 38, no. 16, pp. 4679–4691, May 2018.

[33] S. Mei, F. Liu, and W. Wei, "*Game-Theoretic Engineering Basis and Its Application in Power System*," Science Press, 2020.

[34] R. Jing, M. Wang, Z. H. Zhang, J. Liu, H. Liang, C. Meng, N. Shah, N. Li, and Y. R. Zhao, "Comparative study of posteriori decision-making methods when designing building integrated energy systems with multi-objectives," *Energy and Buildings*, vol. 194, pp. 123–139, Jul. 2019.

[35] *Round Wire Concentric Lay Overhead Electrical Stranded Conductors*, GBT 1179–2017, 2017.

[36] *Typhoon Online*. [Online]. Available: http://www.typhoon.org.cn/.

[37] Z. C. Wei, F. Z. Zhao, J. H. Wang, X. L. Meng, D. M. Chen, Z. J. Ye, and Y. Sheng, "Gridding evaluation index system and method of MV and LV intelligent distribution network," *Power System Technology*, vol. 40, no. 1, pp. 249–255, Jan. 2016.

[38] Z. Zhu, L. Wang, X. Wang, C. Jiang, S. Zhou and K. Gong, "Complementary Operations of Multi-renewable Energy Systems with Pumped Storage," *CSEE Journal of Power and Energy Systems*, vol. 9, no. 5, pp. 1866–1880, Sept. 2023.

[39] J. Cruz, Y. Wu, J. E. Candelo-Becerra, J. C. Vásquez and J. M. Guerrero, "Review of Networked Microgrid Protection: Architectures, Challenges, Solutions, and Future Trends," *CSEE Journal of Power and Energy Systems*, vol. 10, no. 2, pp. 448–467, Sept. 2023.

Wei Tang received the B.S. degree from Huazhong University of Science and Technology, Wuhan, China, in 1992 and the Ph.D. degrees from Harbin Institute of Technology, Harbin, China, in 1998. From 1998 to 2000, she was a post-doctor with Harbin Engineering University. Currently she is a Professor at College of Information and Electrical Engineering, China Agricultural University, Beijing, China. Her research interests include distribution network economic and security operation, distributed generation and active distribution network.

Zhaoqi Wang received the B.S. degree, M.S. degree and Ph.D degree in Electrical Engineering from China Agricultural University, Beijing, China, in 2018, 2020 and 2024, respectively. She is currently an intermediate researcher at the State Grid Energy Research Institute Co., Ltd. Her main research interest includes the equilibrium planning of low-carbon resilient distribution networks.

Lu Zhang received the B.S. degree in Electrical Engineering and the Ph.D. degree in Agricultural Electrification and Automation from China Agricultural University, Beijing, China, in 2011 and 2016, respectively. He was a postdoc in the Department of Electrical Engineering at Tsinghua University From 2017 to 2019. He is currently an Professor at College of Information and Electrical Engineering, China Agricultural University, Beijing, China. His main research interests include hybrid AC/DC distribution network, renewable energy generation, and active distribution networks.

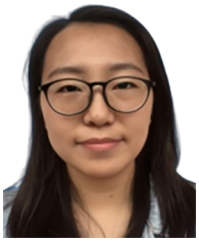

Bo Zhang received the B.S. degree in Electrical Engineering and the Ph.D. degree in Agricultural Electrification and Automation from China Agricultural University, Beijing, China, in 2016 and 2022, respectively. Her research interests include hybrid AC/DC distribution network, renewable energy generation, and economic operation of active distribution network.

Jun Liang received the B.S. degree from the Huazhong University of Science and Technology, Wuhan, China, in 1992, and the M.S. and Ph.D. degrees from China Electric Power Research Institute (CEPRI), Beijing, in 1995 and 1998, respectively. From 1998 to 2001, he was a Senior Engineer with CEPRI. From 2001 to 2005, he was with Imperial College London, U.K., as a Research Associate. From 2005 to 2007, he was with the University of Glamorgan as a Senior Lecturer. He is currently a Professor with the School of Engineering, Cardiff University, Cardiff, U.K. He has been appointed as an Adjunct Professor with the Changsha University of Science and Technology of China and North China Electric Power University since 2014 and 2015. His research interests include HVDC, flexible ac transmission systems, power system stability control, power electronics, and renewable power generation. He is an Editorial Board Member of CSEE JPES.

Keyan Liu received the Ph.D. degree in Electrical Engineering from Beihang University, Beijing, China, in 2007. Dr. Liu was a Postdoctoral Research Fellow with China Electric Power Research Institute, Beijing, from 2012 to 2014. Currently, he is a Senior Researcher with China Electric Power Research Institute. From 2007 to 2012, he was a Senior Researcher with HP Labs China on data-intensive computing algorithm and machine learning. His current research interests are distributed generation, planning and operation analysis of distribution systems, as well as power system computation method and simulation. He has published more than 60 refereed journal and conference papers on the transactions and journals sponsored by IEEE, ACM, and Elsevier.

Wanxing Sheng received the B.Sc., M.Sc., and Ph.D. degrees in Mechanical Engineering from Xi'an Jiaotong University, Xi'an, China, in 1989, 1992, and 1995, respectively. Since 1997, he has been a Full Professor with China Electric Power Research Institute, Beijing, China, where he is currently the Head of the Department of Power Distribution. He is also a Leader of intelligent distribution system and an excellent expert of State Grid Corporation of China, Beijing. He has published over 150 refereed journal and conference papers, and 15 books. His current research interests include power system analysis, renewable energy generation, and grid-connected technologies.